Summer weather becomes more persistent in a 2 °C world

Pfleiderer, Peter; Schleussner, Carl Friedrich; Kornhuber, Kai; Coumou, Dim

published in
Nature Climate Change
2019

DOI (link to publisher)
10.1038/s41558-019-0555-0

document version
Publisher's PDF, also known as Version of record

LETTERS
https://doi.org/10.1038/s41558-019-0555-0

nature climate change

Summer weather becomes more persistent in a 2 °C world

Peter Pfleiderer[1,2,3*], Carl-Friedrich Schleussner[1,2,3], Kai Kornhuber[4,5,6] and Dim Coumou[2,7]

Heat and rainfall extremes have intensified over the past few decades and this trend is projected to continue with future global warming[1–3]. A long persistence of extreme events often leads to societal impacts with warm-and-dry conditions severely affecting agriculture and consecutive days of heavy rainfall leading to flooding. Here we report systematic increases in the persistence of boreal summer weather in a multi-model analysis of a world 2 °C above pre-industrial compared to present-day climate. Averaged over the Northern Hemisphere mid-latitude land area, the probability of warm periods lasting longer than two weeks is projected to increase by 4% (2–6% full uncertainty range) after removing seasonal-mean warming. Compound dry–warm persistence increases at a similar magnitude on average but regionally up to 20% (11–42%) in eastern North America. The probability of at least seven consecutive days of strong precipitation increases by 26% (15–37%) for the mid-latitudes. We present evidence that weakening storm track activity contributes to the projected increase in warm and dry persistence. These changes in persistence are largely avoided when warming is limited to 1.5 °C. In conjunction with the projected intensification of heat and rainfall extremes, an increase in persistence can substantially worsen the effects of future weather extremes.

Extreme weather events are commonly analysed in terms of intensity or frequency but often it is their persistence that leads to the most severe effects. Extended periods of warm and dry weather can strongly affect human health and agriculture and increase risks of wildfires[4]. In 2018, dry and warm conditions in western Europe extended from April to September with only a few short interruptions of cooler and rainy weather[5–7] (see Fig. 1). This persistent dry–warm compound extreme had a devastating effect on agriculture in Germany, with wheat harvests down by 15% (ref. [6]).

Similarly, most damaging flooding events occur following several consecutive days of heavy rainfall[8]. In 2016, a slow-moving low-pressure system remained over Europe for two weeks, resulting in several days of heavy precipitation leading to floods in many municipalities in western Europe[9] (Fig. 1).

Global warming is already increasing the frequency and intensity of heat and rainfall extremes[3], as well as the duration of heat waves[10], and these trends are projected to continue with future warming[11]. However, if and how changes in persistence of local weather conditions might contribute to more severe weather extremes is poorly understood. Some observational studies suggest that summer persistence has increased over recent decades[12–16] but this is so far not supported by modelling studies.

We assess changes in local weather persistence in four general circulation models (GCM) between two ten-year future scenarios at +1.5 °C and +2 °C above pre-industrial and a present-day climate scenario (2006–2015, that is about +1.0 °C above pre-industrial global mean temperatures, GMT). The four atmosphere-only GCMs (NorESM1, MIROC5, ECHAM6-3-LR and CAM-2degree) are run under the HAPPI protocol[17] (half a degree additional warming, prognosis and projected impacts protocol; see Methods). A total 4,000 year per scenario (100 × 10-year runs per model) provide the basis for a statistical analysis of rare events such as periods of extremely persistent weather conditions.

We identify periods of consecutive warm, dry, dry–warm or rain days following the method by Pfleiderer and Coumou[12] (Fig. 1; see also Methods). As illustrated in Fig. 1c, in Berlin in 2018, two uninterrupted warm periods lasting longer than three weeks and several long dry periods are identified. In Paris, three clustered, multi-day rain periods in May 2016 contributed to the Seine flooding in early June (Fig. 1f).

In a warming climate, the number of consecutive days above a given temperature threshold will increase, which leads to an increase in the duration of heat waves with ongoing warming[10,18]. The aim of the persistence concept introduced here, however, is not to identify changes in heat-wave conditions per se but rather to investigate changes in the distribution of warm days relative to the new, warmer climate conditions. Thus, warm days are classified as temperature anomalies that exceed a scenario-dependent, seasonal and grid-cell specific median. This median is computed separately for the present-day, 1.5 °C and 2 °C climate simulations so that in all scenarios half of the days are classified as warm. In this metric, long-term seasonal-mean warming by itself does not lead to an increase in warm persistence.

Unlike for temperature, the classification of what constitutes dry or rainy periods is less dependent on the local background climate state[19]. Therefore, we use the same absolute thresholds for all grid-cells and scenarios to classify dry and rain days: dry days have less than 1 mm and rain days more than 5 mm precipitation.

We also analyse compound dry–warm periods defined as consecutive dry and warm days on the basis of the above metrics. These compound dry–warm events are particularly impact-relevant as they better represent the stress on our environment than do either dry or warm persistence alone[20].

The observed summer-time warm-persistence climatology is well-reproduced by the GCM ensemble (Fig. 2). Regional patterns are generally replicated but some are less pronounced in models compared to observations (compare Fig. 2a,b). As shown in Fig. 2, the enhanced persistence observed over Europe is underestimated

[1]Climate Analytics, Berlin, Germany. [2]Earth System Analysis, Potsdam Institute for Climate Impact Research, Potsdam, Germany. [3]IRI THESys, Humboldt-Universität zu Berlin, Berlin, Germany. [4]Earth Institute, Columbia University, New York, NY, USA. [5]Atmospheric, Oceanic and Planetary Physics, University of Oxford, Oxford, UK. [6]National Centre for Atmospheric Science, Leeds, UK. [7]Department of Water and Climate Risk, IVM, VU University Amsterdam, Amsterdam, the Netherlands. *e-mail: peter.pfleiderer@climateanalytics.org

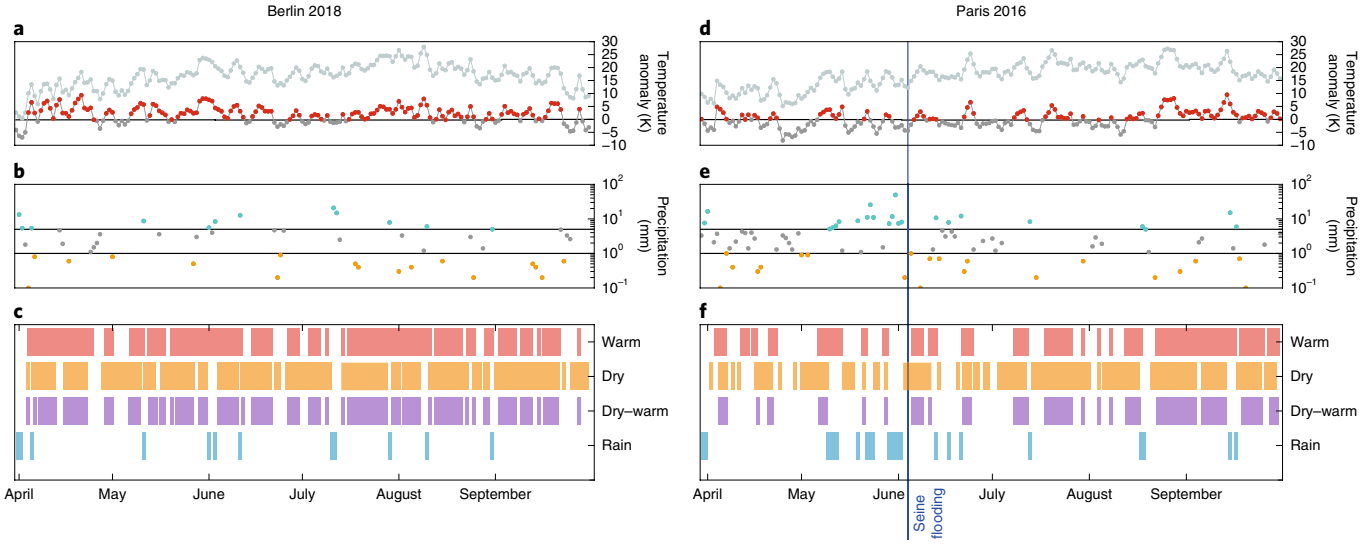

Fig. 1 | Illustration of the persistence metrics. a–f, Persistence derived from the daily gridded observational dataset for Europe (E-OBS). The daily detrended temperature anomaly (**a**,**d**) and daily precipitation (**b**,**e**) time-series for summers in Berlin (52.25° N, 13.25° E) 2018 (**a**–**c**) and Paris (48.75° N, 2.25° E) 2016 (**d**–**f**) are shown. The resulting characterization of the persistence of warm, dry, dry-warm and rain is given in **c** and **f** with coloured bars indicating individual periods (see Methods for details). Thresholds used to classify days into warm, dry and rain days are indicated by black lines. In **a** and **d** the absolute temperature time-series are shown in light grey. For **d**–**f** the date of the Seine flooding (3 June 2016) is indicated by a blue line.

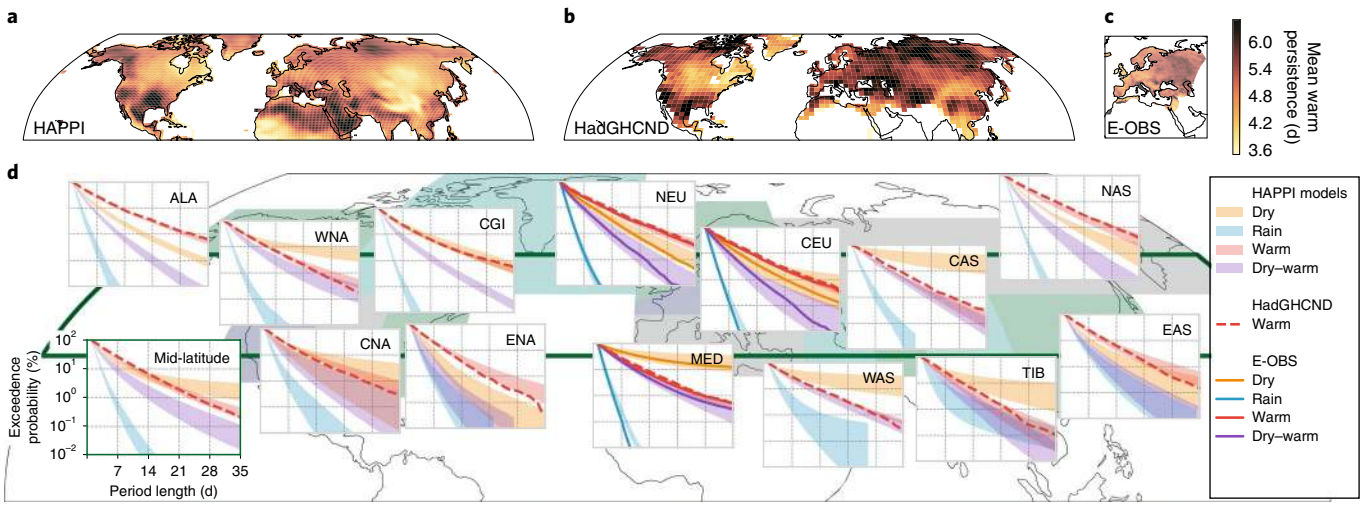

Fig. 2 | Persistence climatology for the NH mid-latitudes in JJA. a–c, Mean period length of persistent warm periods in HAPPI simulations averaged over all 400 runs of the historic 2006–2015 scenario (**a**) and for the observational products HadGHCND (1950–2014, **b**) and E-OBS (1950–2017, **c**). **d**, Exceedance probabilities for warm (red), dry (orange), dry–warm (purple) and rain (blue) persistence for Northern Hemisphere regions (abbreviations follow the IPCC SREX[21], shown in Supplementary Fig. 1). Additionally, persistence averaged over the mid-latitude band (35–60° N) is shown. In each region, the full range of the four models' distributions (all runs of one model are aggregated into one distribution) over the present-day HAPPI simulations is shown by the shaded area. For warm persistence, distributions are shown for HadGHCND observations by a dashed red line. In NEU, CEU and MED, persistence distributions are additionally shown for E-OBS by solid lines.

by the models. For dry and rain persistence, biases are more heterogeneous between models: NorESM1 and CAM4-2degree underestimate dry persistence over Europe, while MIROC5 overestimates dry persistence in northern Europe and ECHAM6-3-LR in southern Europe (Supplementary Fig. 2i–l). Note that the present-day climate scenario in HAPPI (2006–2015) only covers part of the observational record allowing only for a qualitative model validation.

Figure 2d shows the probability of the different persistence metrics to exceed a given period length. Here, for each of the NH SREX regions (Supplementary Fig. 1, region name abreviations follow the IPCC SREX[21]), an aggregated persistence distribution is determined by combining periods identified at grid-cells within the region into one distribution per model. Consistent with previous studies[12], we find that the probability that a warm period persists for one more day increases for longer events (gradient of the curves decreases for longer periods, Fig. 2d). Thus, the more persistent a period is, the more likely it is that it lasts even longer.

In the mid-latitudes, 80% of all warm periods are shorter than a week and 6% exceed two weeks (red curves in Fig. 2d). These exceedance probabilities vary between regions, which is generally well-captured by the climate models.

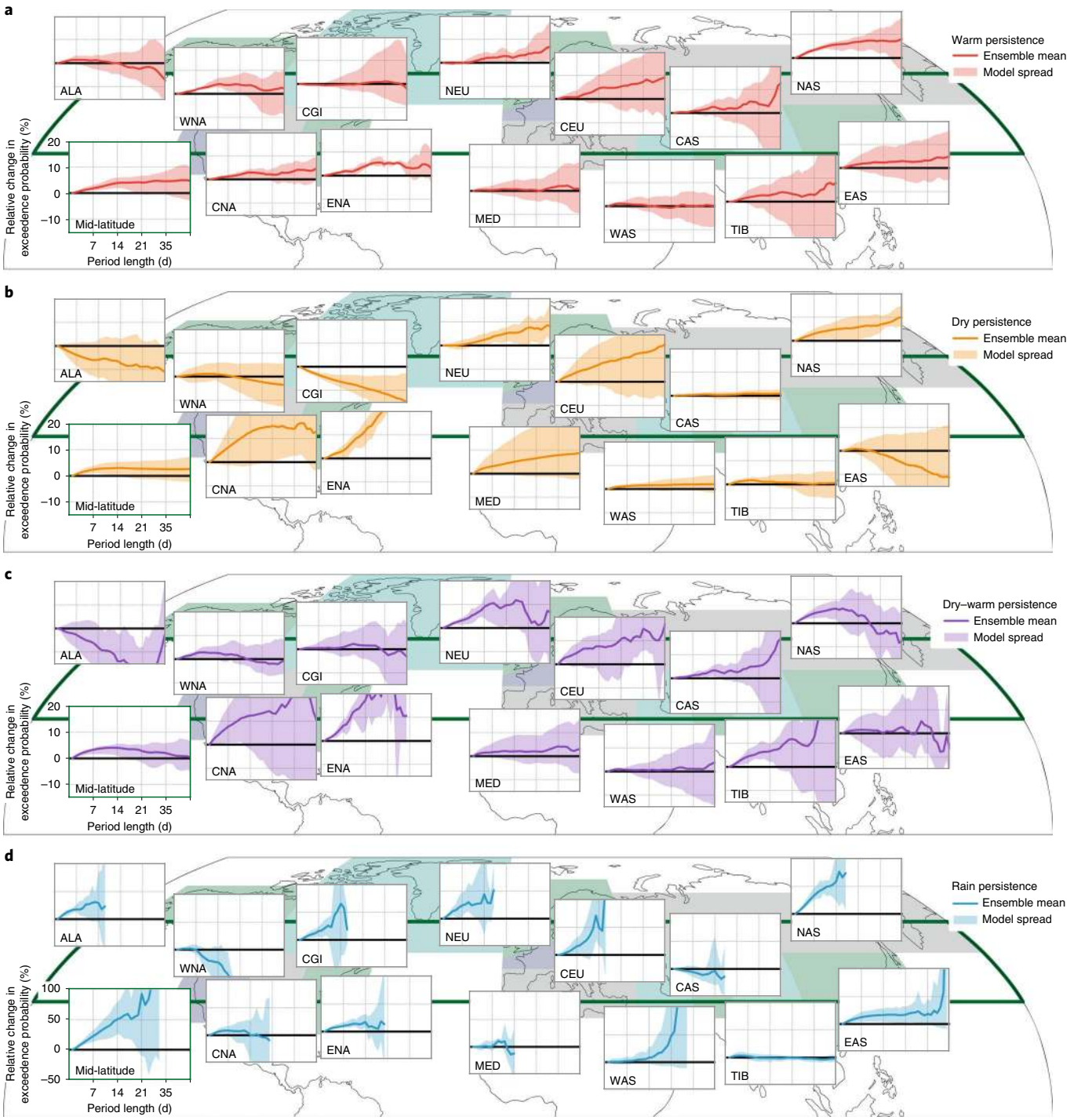

Fig. 3 | Relative change in exceedance probability in JJA in HAPPI models. a–d, Changes of the 2 °C scenario relative to the 2006–2015 scenario are shown for different kinds of persistence: warm (**a**, red), dry (**b**, orange), dry–warm (**c**, purple) and rain (**d**, blue). Note the different scaling for changes in rain persistence (**d**). In each region, the full range of changes in the four models' distributions are shown by the shaded area. The ensemble mean is indicated by a solid line. See Supplementary Tables 1–4 in the Supplementary Information for more details.

Dry and rain persistence strongly vary between regions with month-long dry periods in arid regions (CAS and MED) and only a few periods longer than two weeks in some coastal regions (for example, ENA). In contrast to temperature persistence (with a fixed number of warm days), rainfall persistence also depends on the relative amount of rain and dry days. As rain days are generally rare (see Supplementary Fig. 4), rain periods are limited to less than two weeks in most regions. Periods of consecutive dry–warm days are shorter than warm or dry periods as both criteria need to be fulfilled. Over Europe, for which daily rainfall observations are available, dry, rain and dry–warm persistence are well-represented by the climate models.

The exceedance probability for warm, dry, dry–warm and rain periods consistently increases in a 2 °C world for the Northern Hemisphere mid-latitudes in all HAPPI models (Fig. 3 and Supplementary Tables 1–4). For warm and dry–warm persistence, we

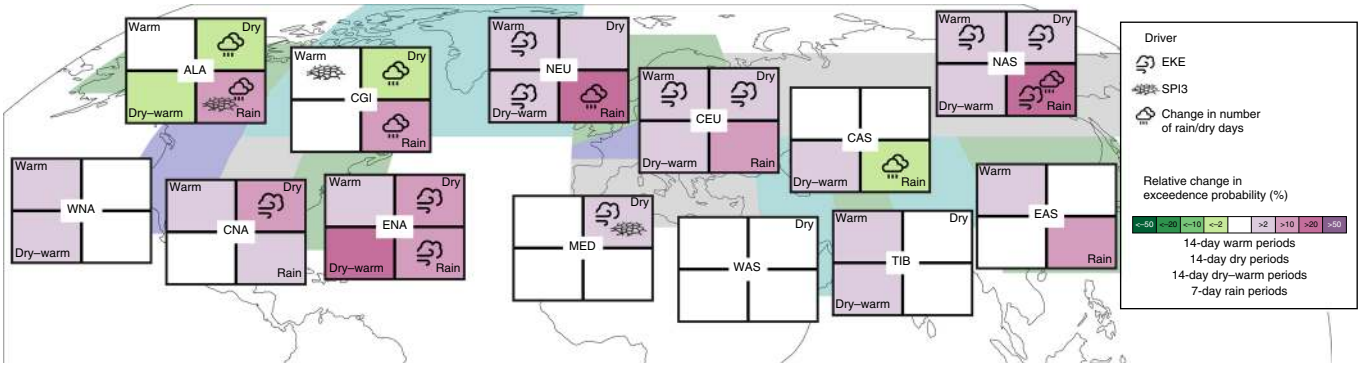

Fig. 4 | Drivers of changes in persistence. For each SREX region (Supplementary Fig. 1) significant increases in persistence are indicated in purple, significant decreases in persistence in green and non-significant changes in white for warm persistence (upper-left), dry persistence (upper-right), dry–warm persistence (lower-left) and rain persistence (lower-right). Changes are considered robust if at least three out of four models show a significant change in persistence ($\alpha = 0.01$) of the same sign. Symbols indicate whether a particular driver (EKE, SPI3 or a change in the number of rain and dry days) can explain the projected changes in persistence (see main text for details).

find a relative increase in exceedance probability of two-week-long periods of 4% (0.5–6%). The increase in warm persistence is most pronounced in northern Asia (NAS), central Europe (CEU) and eastern North America (ENA). For these regions, an increase in dry persistence is found as well.

In regions where warm and dry persistence are projected to increase, compound dry–warm persistence is also increasing. In arid regions (MED, WAS and CAS), dry–warm persistence is limited by warm persistence and thus changes in dry–warm persistence follow those of warm persistence. In central and eastern North America (CNA and ENA) increases in dry–warm persistence appear to be linked to a strong increase in dry persistence.

Rain persistence increases significantly in almost all mid-latitude regions, with long periods increasing most. The average likelihood of week-long rainy conditions increases by 26% (15–37%) in a 2 °C world compared to the present. This increase in rain persistence is especially pronounced for northern Eurasia (NEU, CEU and NAS).

Averaged over the mid-latitude land area and specifically in ENA, CEU, NEU and NAS, dry, rain and warm periods are all projected to be more persistent in a 2 °C world (Fig. 3). As shown in Supplementary Fig. 3, the coincident increase in persistence is also found at the grid-cell level within single models.

The presented long-term changes in warm and dry persistence are probably driven by weakening summer storm tracks, something that is projected by all models. Over the mid-latitudes, warm and dry persistence are longer in months with low eddy kinetic energy (EKE), which is a proxy for storm track activity. For each model and region, we checked the correlation between the length of the longest period in each month and monthly EKE. This correlation is negative for most regions and, in combination with a projected decrease in EKE, this can partially explain the trend towards longer warm and dry persistence. We consider EKE to be a driver of a change in persistence if at least three models project a significant change in persistence that matches the expected EKE forcing (more details in the Supplementary Information, especially Supplementary Fig. 8). As shown in Fig. 4, EKE explains most changes in persistence projected for regions affected by the North Atlantic jetstream (ENA, MED, CEU and NEU). These findings are consistent with previous studies showing that weather persistence in the mid-latitudes is tightly linked to large-scale atmospheric circulation such as the jetstream or storm tracks[22,23] and that storm track activity is weakening in boreal summer[24,25].

Changes in the water cycle due to enhanced evapotranspiration and water-holding capacity of the atmosphere lead to changes in the number of dry and rain days (compare Supplementary Fig. 5). To test how the change in the number of rain and dry days affects rain and dry persistence, we create synthetic future weather time-series by randomly adding or removing dry and rain days to the historic time-series to match the amount of dry and rain days projected for the 2 °C scenario. As shown in Supplementary Fig. 6, the increase in rain persistence in the high latitudes can partly be explained by an increase in the number of rain days. However, overall, the changes in dry and rain days can only explain half of the actually projected changes in persistence (compare Supplementary Fig. 7).

Land–atmosphere interactions might also influence the persistence of warm and dry periods. During warm periods, a lack of soil moisture hinders evaporative cooling and cloud formation, which can further increase temperatures[26,27]. Long-lasting warm and dry periods thereby favour subsequent warm and dry days, which is expressed by a negative correlation of warm and dry persistence with the standardized precipitation index of the preceding 3 months (SPI3; see Supplementary Fig. 9). In HAPPI projections, summer SPI3 increases in the NH mid-latitudes, wetting the soils; thus land–atmosphere interactions are unlikely to play a role in the projected increases in dry persistence. The Mediterranean (MED) forms an exception: here, SPI3 decreases and this soil drying, together with the effect from weakening storm tracks, probably contributes to an increase in dry persistence.

Our analysis of potential drivers of persistence suggests that the weakening of summer storm tracks is an important driver of increased persistence in the mid-latitudes (see Fig. 4). Changes in the hydrological cycle only have limited explanatory power. The persistent summer 2018 was linked to a slow-moving stationary wave[5] and further research will analyse the underlying circulation patterns of extremely persistent weather conditions to further improve our understanding of changes in summer weather persistence.

We find a projected lengthening of dry and warm periods in important breadbaskets such as central North America (CNA) and Europe (NEU/CEU). As long-lasting warm and dry periods have severe impacts on agriculture[6] and extreme weather events are already negatively affecting crop production[28], the lengthening of warm and dry periods in these regions imposes a risk for food production. Furthermore, the substantial increase in the probability of week-long heavy rain enhances the risk of flooding.

We showed that changes in the clustering of relatively warm summer days (warm relative to the scenario mean warming) leads to longer uninterrupted warm periods (Fig. 3a). On top of this dynamic change, these warm periods will become more intense due to purely thermodynamic increases in global mean tempera-

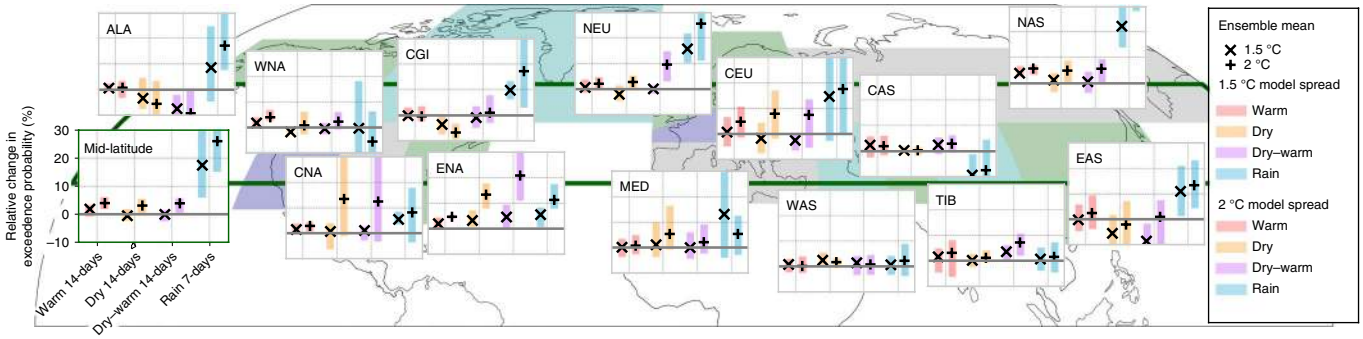

Fig. 5 | Relative change in exceedance probability distributions for 2 °C and 1.5 °C worlds versus 2006–2015 in HAPPI models. Changes are shown for SREX regions and the mid-latitudes (Supplementary Fig. 1) for the probability of persistent periods exceeding 14 warm days (red), 14 dry days (orange), 14 dry–warm days (purple) and 7 rain days (blue). In each region, the full range of changes of the four models' distributions are shown by the shaded area. The ensemble mean is highlighted by an 'x' for the 1.5 °C world and by a '+' for the 2 °C world.

ture. For a future warming of +1 °C compared to present-day, we find that warm periods longer than two weeks will become 1.5 °C warmer on average. Likewise, global warming increases the intensity of heavy precipitation events and the drying potential of soils during warm periods[3].

Most of the projected increases in persistence can be avoided by limiting warming to 1.5 °C (Fig. 5). For central North America (CNA) and central Europe (CEU) a relative increase of 10% in dry–warm persistence is projected for 2 °C but no change for the 1.5 °C scenario. This suggests a nonlinear dependence of dry–warm persistence with GMT. Rain persistence increases almost everywhere, also under 1.5 °C, scaling roughly linearly with GMT.

Our analysis shows that summer weather becomes more persistent, with global warming increasing risks associated with long-lasting heat waves, droughts, rain periods and compound hot–dry extremes.

Online content

Any methods, additional references, Nature Research reporting summaries, source data, statements of code and data availability and associated accession codes are available at https://doi.org/10.1038/s41558-019-0555-0.

Received: 14 January 2019;
Published online: 19 August 2019

References

1. Coumou, D., Robinson, A. & Rahmstorf, S. Global increase in record-breaking monthly-mean temperatures. *Climatic Change* **118**, 771–782 (2013).
2. Lehmann, J., Mempel, F. & Coumou, D. Increased occurrence of record-wet and record-dry months reflect changes in mean rainfall. *Geophys. Res. Lett.* **45**, 13468–13476 (2018).
3. IPCC *Climate Change 2013: The Physical Science Basis* (eds Stocker, T. F. et al.) (Cambridge Univ. Press, 2013).
4. Petoukhov, V. et al. Alberta wildfire 2016: apt contribution from anomalous planetary wave dynamics. *Sci. Rep.* **8**, 12375 (2018).
5. Kornhuber, K. et al. Extreme weather events in early summer 2018 connected by a recurrent hemispheric wave-7 pattern. *Environ. Res. Lett.* **14**, 054002 (2019).
6. *Erntebericht 2018* (BMEL, 2018); https://www.bmel.de/DE/Landwirtschaft/Pflanzenbau/Ackerbau/_Texte/Ernte2018.html
7. *Deutschlandwetter im Sommer 2018* (DWD, 2018); https://www.dwd.de/DE/presse/pressemitteilungen/DE/2018/20180830_deutschlandwetter_sommer.html
8. Stadtherr, L., Coumou, D., Petoukhov, V., Petri, S. & Rahmstorf, S. Record Balkan floods of 2014 linked to planetary wave resonance. *Sci. Adv.* **2**, e1501428 (2016).
9. van Oldenborgh, G. J. et al. Rapid attribution of the May/June 2016 flood-inducing precipitation in France and Germany to climate change. *Hydrol. Earth Syst. Sci. Discuss.* https://doi.org/10.5194/hess-2016-308 (2016).
10. Perkins-Kirkpatrick, S. E. & Gibson, P. B. Changes in regional heatwave characteristics as a function of increasing global temperature. *Sci. Rep.* **7**, 1–12 (2017).
11. O. Hoegh-Guldberg, et al. in *Global Warming of 1.5 °C* (eds Masson-Delmotte, V. et al.) 175–312 (IPCC, WMO, in the press).
12. Pfleiderer, P. & Coumou, D. Quantification of temperature persistence over the Northern Hemisphere land-area. *Clim. Dynam.* **51**, 627–637 (2018).
13. Francis, J. A., Skific, N. & Vavrus, S. J. North American weather regimes are becoming more persistent: is Arctic amplification a factor? *Geophys. Res. Lett.* **45**, 11,414–11,422 (2018).
14. Horton, D. E. et al. Contribution of changes in atmospheric circulation patterns to extreme temperature trends. *Nature* **522**, 465–469 (2015).
15. Hoffmann, P. Enhanced seasonal predictability of the summer mean temperature in Central Europe favored by new dominant weather patterns. *Clim. Dynam.* **50**, 2799–2812 (2018).
16. Alvarez-Castro, M. C., Faranda, D. & Yiou, P. Atmospheric dynamics leading to west European summer hot temperatures since 1851. *Complexity* **2018**, 1–10 (2018).
17. Mitchell, D. et al. Half a degree additional warming, prognosis and projected impacts (HAPPI): background and experimental design. *Geosci. Model Dev.* **10**, 571–583 (2017).
18. Dosio, A., Mentaschi, L., Fischer, E. M. & Wyser, K. Extreme heat waves under 1.5 °C and 2 °C global warming. *Environ. Res. Lett.* **13**, 054006 (2018).
19. Zhang, X. et al. Indices for monitoring changes in extremes based on daily temperature and precipitation data. *WIREs Clim. Change* **2**, 851–870 (2011).
20. Zscheischler, J. et al. Future climate risk from compound events. *Nat. Clim. Change* **8**, 469–477 (2018).
21. IPCC *Managing the Risks of Extreme Events and Disasters to Advance Climate Change Adaptation* (eds Field, C.B. et al.) (Cambridge Univ. Press, 2012).
22. Coumou, D., Di Capua, G., Vavrus, S., Wang, L. & Wang, S. The influence of Arctic amplification on mid-latitude summer circulation. *Nat. Commun.* **9**, 2959 (2018).
23. Mann, M. E. et al. Projected changes in persistent extreme summer weather events: the role of quasi-resonant amplification. *Sci. Adv.* **4**, eaat3272 (2018).
24. Coumou, D., Lehmann, J. & Beckmann, J. The weakening summer circulation in the Northern Hemisphere mid-latitudes. *Science* **348**, 324–327 (2015).
25. Lehmann, J., Coumou, D., Frieler, K., Eliseev, A. V. & Levermann, A. Future changes in extratropical storm tracks and baroclinicity under climate change. *Environ. Res. Lett.* **9**, 084002 (2014).
26. Hirschi, M. et al. Observational evidence for soil-moisture impact on hot extremes in southeastern Europe. *Nat. Geosci.* **4**, 17–21 (2011).
27. Donat, M. G., Pitman, A. J. & Angélil, O. Understanding and reducing future uncertainty in midlatitude daily heat extremes via land surface feedback constraints. *Geophys. Res. Lett.* **45**, 10,627–10,636 (2018).
28. Lesk, C., Rowhani, P. & Ramankutty, N. Influence of extreme weather disasters on global crop production. *Nature* **529**, 84–87 (2016).

Acknowledgements

The authors would like to thank the HAPPI initiative and all participating modelling groups that have provided data. This research used science gateway resources of the National Energy Research Scientific Computing Center, a Science User Facility supported by the Office of Science of the US Department of Energy under contract no. DE-AC02-05CH11231. We thank the Met Office Hadley Centre for providing the HadGHCND dataset. We acknowledge the E-OBS dataset from the EU-FP6 project ENSEMBLES (http://ensembles-eu.metoffice.com) and the data providers in the ECA&D

project (http://www.ecad.eu). P.P. and C.-F.S. acknowledge support by the German Federal Ministry of Education and Research (01LN1711A). K.K. is supported by the UK NERC, NCAS and NERC grant nos NE/P006779/1 and NE/N018001/1. This work was supported by the BMBF (grant no. 01LN1304A to D.C.) and the NWO (grant no. 016.Vidi.171011 to D.C.).

Author contributions

P.P., C.-F.S., K.K. and D.C. conceived the study. P.P. analysed the data. P.P. wrote the manuscript with contributions from all authors.

Competing interests

The authors declare no competing interests.

Additional information

Supplementary information is available for this paper at https://doi.org/10.1038/s41558-019-0555-0.

Reprints and permissions information is available at www.nature.com/reprints.

Correspondence and requests for materials should be addressed to P.P.

Peer review information: *Nature Climate Change* thanks Peter Gibson and the other, anonymous, reviewer(s) for their contribution to the peer review of this work.

Methods

HAPPI simulations. We analyse HAPPI simulations of four atmosphere-only GCMs: NorESM1, MIROC5, ECHAM6-3-LR and CAM-2degree. The HAPPI protocol includes a current climate scenario (2006–2015) and two future scenarios for 1.5 °C and 2 °C global mean temperature relative to pre-industrial levels[17]. For each scenario, an ensemble of 100 runs per model is analysed. Future sea surface temperature (SST) patterns are obtained by adding an SST change pattern from CMIP5 simulations on 2006–2015 SST patterns. Future sea-ice coverage patterns are based on a regression between sea-ice coverage and SST, which is then applied on future SST patterns.

Observations and reanalysis. For model evaluation, we use the HadGHCND dataset, which is based on daily observed temperatures from 1950 to 2014 aggregated on a 3.75°×2.5° grid[29] and the daily gridded observational dataset for Europe (E-OBS), which includes daily temperatures and precipitations from 1950 to 2018 on a 0.5°×0.5° grid[30]. Due to a lack of data coverage in the tropics and most parts of the Southern Hemisphere, our analysis is restricted to the Northern Hemispheric extra-tropics.

We additionally use the Global Precipitation Climatology Centre (GPCC) v.7 monthly precipitation observations to calculate SPI3 over the observational record[31].

We use the ERA-Interim reanalysis to calculate EKE over the period 1979–2017 (ref. [32]).

Warm persistence. The quantification of warm persistence follows the method outlined by ref. [12]. At each grid-cell and in each season, days are classified into cold and warm days relative to the state of seasonal warming. Periods of consecutive warm or cold days are then aggregated into persistence distributions for each grid-cell. For HAPPI simulations, all three scenarios are treated separately. As each ten-year run is expected to represent a stationary climate we subtract the daily climatology of the scenario for each run to get temperature anomalies relative to the climate scenario. HadGHCND and E-OBS observations are detrended on a daily basis: multi-year time-series for all 365 days of a year (for example, all 1 January) are linearly detrended and the climatological mean is subtracted.

Precipitation persistence. For the analysis of persistence of dry periods, we classify all days with precipitation lower than 1 mm at the grid-cell level as dry days following ref. [33]. Instead of classifying all days that are not dry as rain days, we only consider days with more than 5 mm precipitation to be rain days.

Using the classification of warm and dry days (see above), we define compound dry–warm persistence through periods of consecutive days of warm and dry conditions.

Eddy kinetic energy. We study links between changes in storm track activity and persistence using EKE as a proxy for storm track activity. EKE is based on daily horizontal wind fields filtered with a 2.5–6-day bandpass filter[34]. The EKE is calculated as:

$$\mathrm{EKE} = \frac{1}{2}(v^2 + u^2)$$

where u and v are the bandpass filtered longitudinal and meridional wind speeds at the 850 mbar level.

Standardized precipitation index. We take the SPI3 as an index for soil moisture[35]. We calculate the SPI3 using the R-package standardized precipitation evapotranspiration index (SPEI[36]).

Data availability

The observational data and HAPPI simulations that support the findings of this study are publicly available online at https://www.metoffice.gov.uk/hadobs/hadghcnd, https://www.ecad.eu/download/ensembles/download.php and https://portal.nersc.gov/c20c/data.html.

Code availability

Python scripts used for the analysis are available on github.com/peterpeterp/persistence_in_HAPPI.

References

29. Donat, M. G. et al. Global land-based datasets for monitoring climatic extremes. *Bull. Am. Meteorol. Soc.* **94**, 997–1006 (2013).
30. Haylock, M. R. et al. A European daily high-resolution gridded data set of surface temperature and precipitation for 1950-2006. *J. Geophys. Res. Atmos.* **113**, D20119 (2008).
31. Meyer-Christoffer, A., Becker, A., Finger, P., Schneider, U. & Ziese, M. *GPCC Climatology Version 2018 at 1.0°* (GPCC, 2018); https://doi.org/10.5676/DWD_GPCC/CLIM_M_V2018_100.
32. Dee, D. P. et al. The ERA-Interim reanalysis: configuration and performance of the data assimilation system. *Q. J. R. Meteorol. Soc.* **137**, 553–597.
33. Zolina, O., Simmer, C., Belyaev, K., Gulev, S. K. & Koltermann, P. Changes in the duration of European wet and dry spells during the last 60 years. *J. Clim.* **26**, 2022–2047 (2013).
34. Murakami, M. Large-scale aspects of deep convective activity over the GATE area. *Mon. Weather Rev.* **107**, 994–1013 (1979).
35. McKee, T. B., Doesken, N. J. & Kleist, J. The relationship of drought frequency and duration to time scales. In *Proc. Eighth Conference on Applied Climatology* 179–184 (American Meteorological Society, 1993).
36. Vicente-Serrano, S. M., Beguería, S. & López-Moreno, J. I. A multiscalar drought index sensitive to global warming: the standardized precipitation evapotranspiration index—SPEI. *J. Clim.* **23**, 1696–1718 (2010).